Food Chemistry: X 24 (2024) 102028

Contents lists available at ScienceDirect

Food Chemistry: X

journal homepage: www.sciencedirect.com/journal/food-chemistry-x

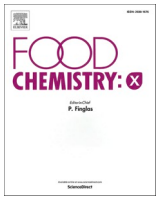

The effect of pH on structural properties and interaction mechanisms of zein/epicatechin gallate complexes

Xiujuan Chen [a], Kaili Nie [a], Xuejun Huang [a], Hao Li [a,b], Yexu Wu [c], Yi Huang [a], Xiaoqiang Chen [a,b,*]

[a] Cooperative Innovation Center of Industrial Fermentation (Ministry of Education & Hubei Province), Key Laboratory of Fermentation Engineering (Ministry of Education), National "111" Center for Cellular Regulation and Molecular Pharmaceutics, Hubei University of Technology, Wuhan 430068, China
[b] School of Life Sciences, Hubei University, Wuhan 430062, China
[c] Hubei Provincial Key Laboratory of Yeast Function, Angel Yeast Co. Ltd., Yichang 443000, China

ARTICLE INFO

Keywords:
Zein
Epicatechin gallate
pH
Structural changes
Interaction mechanism

ABSTRACT

This study aimed to investigate the effects of pH on the structural properties and interaction mechanisms of zein/epicatechin gallate (ECG) complexes. QCM-D data demonstrated that the binding capacity of ECG to zein was significantly higher under alkaline condition (pH 9) compared to neutral and acidic conditions ($p < 0.05$). Molecular docking analysis revealed that the formation of zein/ECG complexes was primarily driven by hydrogen bonds, van der Waals forces, and hydrophobic interactions. Fourier transform infrared spectroscopy indicated changes in secondary structure of zein. Additionally, these structural changes resulted in a decrease in content of free sulfhydryl groups while increasing solubility and antioxidant activity. Furthermore, melting temperature of zein/ECG complexes decreased after treatments at pH 3, 5, and 9, while it increased at pH 1 and 7. These findings underscore the significance of pH in ECG and zein interaction, offering valuable insights for the development of zein/ECG complexes as food additives.

1. Introduction

Catechins, primarily composed of epigallocatechin gallate (EGCG), epicatechin gallate (ECG), epicatechin, and epigallocatechin, are significant polyphenols found in tea (Yang et al., 2024). ECG is a water-soluble active compound that ranks second in content after EGCG. Recently, it has been extensively studied and demonstrated to possess various biological activities, including antioxidants (Zhu et al., 2023) and antibacterial properties (Wang et al., 2022). Furthermore, ECG is sensitive to environmental factors such as heat, oxygen, and pH due to its multiple phenolic hydroxyl groups, which contribute to its low bioavailability (Zhu et al., 2023). Common strategies to enhance its stability include modifying ECG with food proteins (Guo et al., 2024).

Zein, derived from maize endosperm, exhibits low water solubility due to its high content of nonpolar amino acids (Giteru et al., 2021). It is commonly utilized to encapsulate and deliver various polyphenolic compounds such as EGCG (Dong et al., 2023; Vale et al., 2024), proanthocyanidin (Li et al., 2023), and isoquercetin (Yue et al., 2024). Multifunctional zein-polyphenol complexes have been developed through the interactions explored in various research studies. Composite zein nanoparticles modified with gallic acid demonstrated improved emulsion stability and slowed the oxidation of encapsulated algal oil (Xu et al., 2023). Additionally, zein/tannic acid composite nanoparticles improved the stability and bacteriostatic activity of Pickering emulsions (Fan et al., 2024). Furthermore, it has been reported that zein hydrogels mediated by EGCG formation effectively inhibited lipid oxidation in beef (Ruan et al., 2022). Moreover, polyphenols can modify the structure and properties of zein. For instance, zein/chlorogenic acid and zein/gallic acid conjugates exhibited greater dispersibility, thermal stability, and antioxidant activity compared to zein alone (Xu et al., 2022b). Another study found that a zein/resveratrol conjugate similarly displayed enhanced emulsifying and antioxidant properties (Ren et al., 2022).

Additionally, various environmental factors influence protein-polyphenol interactions. pH is a critical factor as it alters the surface charge of both proteins and polyphenols (Chen et al., 2024). Indeed, Wang, Tang, et al. (2022c) found that ferulic acid exhibited the strongest

* Corresponding author at: Cooperative Innovation Center of Industrial Fermentation (Ministry of Education & Hubei Province), Key Laboratory of Fermentation Engineering (Ministry of Education), National "111" Center for Cellular Regulation and Molecular Pharmaceutics, Hubei University of Technology, Wuhan 430068, China
E-mail address: biomed528@163.com (X. Chen).

https://doi.org/10.1016/j.fochx.2024.102028
Received 10 October 2024; Received in revised form 15 November 2024; Accepted 19 November 2024
Available online 22 November 2024

binding stability to zein at pH 9. The zein/anthocyanin composite nanoparticles prepared at pH 2 and pH 4 exhibited greater protection against anthocyanins compared to those prepared at pH 7 (Li et al., 2023). It was also noted that the binding tendency of soybean glycine and β-glycine to EGCG was primarily dependent on pH (Yang et al., 2020), with the strongest binding occurring at pH 7.

Moreover, the quartz crystal microbalance with dissipation monitoring (QCM-D) is an effective sensing technology that leverages the piezoelectric properties of quartz crystals. It provides valuable information on real-time substance binding capacities of substances through the adsorption of a monomolecular layer on the sensor surface (Setiowati et al., 2021). The QCM-D technique has been extensively employed to investigate the interactions between biomolecules and small molecules (Ye et al., 2022). Additionally, spectroscopic analysis and molecular modeling have emerged as powerful tools for studying the structural properties of proteins and their interaction mechanisms with small molecules (Bu et al., 2024).

The effect of pH on zein's interaction with small molecules and its application as a delivery substrate for active substances has been extensively documented. Especially as the most abundant catechin in tea, EGCG has been reported to interact with zein multiple times (Liu et al., 2017; Liu et al., 2021; Vale et al., 2024). However, the mechanism, structure, and bioactivity of zein's interaction with ECG have been scarcely documented to date. Consequently, zein and zein/ECG complexes were successfully prepared at various pH levels. The structural and physicochemical properties of these were thoroughly investigated using a range of spectroscopic methods, including UV–visible (UV–vis) absorption, Fourier-transform infrared (FT-IR) spectroscopy, and fluorescence spectroscopy. Additionally, the binding capacity of ECG to zein was systematically analyzed for the first time using highly sensitive and quantitative QCM-D at pH levels of 1, 3, 5, 7, and 9. Furthermore, molecular docking was employed to examine the binding energy and intermolecular forces between ECG and zein. This study may provide valuable insights into the interactions of zein with other small molecules and contribute to the design of zein-based systems for the protection and delivery of active substances.

2. Materials and methods

2.1. Materials

Zein (purity ≥92 %) was acquired from Shanghai yuanye Bio-Technology Co., Ltd. ECG (purity ≥98 %) was purchased from Taiyo Green Power Co., Ltd. Sodium dodecyl sulfate (SDS), ethylenediaminetetraacetic acid (EDTA), 5,5′-dithiobis-(2-nitrobenzoic acid) (DTNB), 2,2-azino-bis(3-ethylbenzthiazoline)-6-sulfonic acid (ABTS), 1,10-diphenyl-2-picrylhydrazyl (DPPH), pepsin (P7000, porcine, 800–2500 U/mg), and trypsin (porcine, ≥ 250 NFU/mg) were bought from Sigma-Aldrich (China). Bile salts NO. 3 was purchased from Sinopharm Chemical Reagent Co., Ltd. Bovine serum albumin (BSA) was obtained from Biofroxx (China).

2.2. Sample preparation

The preparation of zein/ECG complexes was based on a method of Liu et al. (2017) with appropriate adjustments. Briefly, 1 g of zein and 0.2 g of ECG powder were respectively placed in sealed bottles and dissolved in 50 mL of a 70 % (*v*/v) aqueous ethanol solution. The solutions were subjected to ultrasound for two minutes, then immediately sealed and stirred at room temperature for one hour. Next, they were mixed to form a composite solution with zein at 10 mg/mL and ECG at 2 mg/mL, respectively. The pH was adjusted to 1, 3, 5, 7, and 9 using 0.1 M HCl and NaOH. Then, the mixture was stirred at room temperature without oxygen for 12 h. Finally, zein/ECG complexes powder was obtained through freeze-drying. The resulting products were sequentially named ZE-1, ZE-3, ZE-5, ZE-7, and ZE-9. Zein solution without ECG was used as a control with the same treatment, and the obtained powders were named Z-1, Z-3, Z-5, Z-7, and Z-9, respectively.

2.3. Sodium dodecyl sulfate-polyacrylamide gel electrophoresis (SDS-PAGE)

The molecular weight of all samples was assessed according to the procedure of Tan et al. (2021) with slight adjustments. The specific steps were as follows:

First, a 1 mg/mL solution of each sample was prepared, respectively. Then, it was mixed with a 1:1 (*v*/v) sodium dodecyl sulfate-reducing buffer and boiled for 3 min. Subsequently, 5 μL of the standard protein (10–250 KDa, Polymeric, Beijing, China) and 20 μL of the boiled sample solution were added dropwise to the 4 % concentrating gel and 15 % separating gel made of polyacrylamide, respectively. The electrophoresis was executed, and then Blue R-250 was used to stain for around 2 h. Finally, the gel was decolorized with a 6:3:1 (v/v/v) mixture of ultrapure water/methanol/glacial acetic acid.

2.4. UV–vis absorption spectroscopy

Each sample solution was made of 70 % (*v*/v) aqueous ethanol. The UV–visible absorption spectroscopy was obtained using the UV spectrophotometer (UV-2600i, Shimadzu, Japan) in the range of 200–500 nm.

2.5. FT-IR spectroscopy

All samples were sequentially analyzed using an iS10 FT-IR spectrometer (Thermofisher, America) within the range of 4000–525 cm^{-1}. The PeakFit v4 software (SPSS Inc., Chicago, IL, USA) was involved in calculating the contents of the second structure of zein.

2.6. Intrinsic fluorescence spectroscopy

Each sample solution (1 mg/mL) was prepared using 70 % (*v*/v) aqueous ethanol. F-7000 spectrofluorometer (Hitachi, Japan) was utilized to acquire intrinsic fluorescence spectroscopy data. The excitation and emission wavelengths were set at 290 nm and ranged from 300 to 500 nm, respectively.

2.7. Scanning electron microscopy (SEM)

A small amount of each sample powder was evenly applied to the conductive adhesive and then sprayed with gold. The surface morphological features were examined using a scanning electron microscope (JSM-6390LV, Japan).

2.8. QCM-D measurement

QCM-D experiment was referred to as the method by Setiowati et al. (2021) using the Q-Sense (Biolin Scientific AB, Gothenburg, Sweden) with a gold sensor. First, zein and ECG solutions were prepared using 70 % (*v*/v) aqueous ethanol, and the pH was adjusted to 1, 3, 5, 7, and 9, respectively. The gold sensor was placed in a 5:1:1 (v/v/v) mixture of ultrapure water/25 % ammonia/30 % hydrogen peroxide with a water bath at 75 °C for 10 min. It was cleaned in ultrapure water, dried with nitrogen, loaded into the QCM-D system, and then pumped with 70 % (v/v) aqueous ethanol. After stabilizing the frequency and dissipation baselines, zein solutions with varying pH were passed through until the gold sensor adsorption reached saturation. Then, 70 % (v/v) aqueous ethanol was passed to wash away the weakly adsorbed zein. Subsequently, changes in frequency and dissipation were observed when the ECG solutions of the corresponding pH were flowing. Finally, it was washed with 70 % (v/v) aqueous ethanol until the frequency stabilized.

Moreover, the coupled mass was calculated by the equation $\Delta m =$

−c/n * ΔF, where n and c represent the number of resonance overtones and the mass sensitivity constant (18 ng cm^{-2} Hz^{-1}), respectively (Setiowati et al., 2021).

2.9. Molecular docking

The natural zein structure has not been determined, so homology modeling was used to generate a structural model (Yue et al., 2024). The amino acid sequence (UniProtKB: Q9SYT3) was retrieved from https://www.uniprot.org/. The structural modeling of zein was established through https://alphafold.ebi.ac.uk (**Fig. 5B**). Then the model's reasonableness was evaluated using PROCHECH (https://saves.mbi.ucla.edu). Meanwhile, the ECG structure was acquired from PubChem (https://pubchem.ncbi.nlm.nih.gov). The interaction ECG with zein was probed with AutoDock 4, and the interface input files were generated using AutoDock Tools 1.5.6. Finally, Discovery Studio 4.5 and Pymol 2.5 were used to analyze the docking results.

2.10. Free sulfhydryl group (SH) measurement

The SH content of each sample was quantified following the method of Hong et al. (2024) with slight enhancements. Briefly, sample powders were dissolved in 70 % (*v*/v) aqueous ethanol. Then, 1 mL (3 mg/mL) of sample solution was mixed with 5 mL of Tris-glycine buffer (0.5 % SDS, 0.086 M Tris, 0.04 M EDTA, and 0.09 M glycine, pH 8.0), followed by the addition of 50 μL of Ellman's reagent (4 mg/mL). Subsequently, the mixture was homogenized and allowed to react for 15 min at 25 °C in a water bath. Then, the absorbance values at 412 nm were examined. Meanwhile, a control without Ellman's reagent was treated similarly. The equation for calculating the SH content in μmol/g is: SH content (μmol/g) = 73.53 * A * D / C. Here, A, D, and C signal the absorbance of the sample minus the control, the dilution coefficient, and the concentration of samples, respectively.

2.11. Differential scanning calorimetric (DSC)

Melting temperatures of all samples were investigated using a Mettler-Toledo DSC (TA Instrument, Switzerland). Accurately weighed 3-5 mg samples were taken in the crucible. The temperature ranged from 25 °C to 150 °C at a heating rate of 10 °C/min. Meanwhile, a blank crucible was placed into a control. The DSC thermograms and correlation temperatures were analyzed using TA software.

2.12. Solubility and turbidity evaluation

The solubility and turbidity were measured with slight adjustments, following the methodology outlined in Xu et al. (2022a). In brief, the sample solution (20 mg/mL) was prepared using ultrapure water and stirred continuously for 1 h. Next, it was centrifuged at 10000 rpm for 15 min. The protein in the supernatant was quantified using the Coomassie Brilliant Blue method, with BSA as the standard. Meanwhile, the sample solution (1 mg/mL) was stirred continuously for 1 h. The absorbance values at 600 nm were measured to assess the turbidity.

2.13. Measurement of antioxidant activity

DPPH and ABTS radical scavenging activities were examined following the procedure outlined by Ren et al. (2022) with slight modifications. 0.5 mL (0.5 mg/mL) of the sample solution and 1 mL of DPPH solution (0.1 mM) were combined, mixed, and allowed to react for 1 h in the dark. Subsequently, the absorbance values at 517 nm were examined. Meanwhile, 0.5 mL (0.5 mg/mL) of the sample solution and 1 mL of ABTS radical working solution were combined, mixed, and allowed to react for 0.5 h in the dark. The absorbance values at 734 nm were then determined.

2.14. In vitro digestion

In vitro, simulated digestion was estimated following the procedure of Zhao et al. (2022) with slight improvements.

For simulated gastric digestion, 20 mL of the sample solution (0.5 mg/mL) and 20 mL of pepsin (3.2 mg/mL) were accurately measured and mixed. The pH was then altered to 2.5 using 0.1 M HCl. Subsequently, the mixed solution was reacted at 37 °C for 120 min in a water bath with continuous stirring. During the process, samples of the digested solution were collected at 30, 60, 90, and 120 min into the reaction.

For simulated intestinal digestion, 30 mL of the finished gastric digests were accurately pipetted, and the pH was changed to 7 by adding 0.25 M NaOH. Subsequently, 3.5 mL of bile salt (53.57 mg/mL), 1.5 mL of salt solution, and 2.5 mL of pancreatic lipase (24 mg/mL) were added. The reaction was continued for 120 min at 37 °C in a water bath with continuous stirring. In this process, the pH value was maintained at 7 by supplementing with NaOH. Sampling was conducted in the same manner as for simulated gastric digestion.

The digests were centrifuged at 10,000 rpm and 4 °C for 30 min. The quantification of proteins in the supernatant was performed as described in section **2.12** of this study. The equation for calculating D_t (%) = (m-m_t)/m*100 %, where D_t and m_t denote the digestibility and protein mass in the digest supernatant at digestion time t, respectively, and m represents the sample weight.

2.15. Statistical analysis

Data was analyzed using Origin 2019, while the difference ($p < 0.05$) was assessed with a one-way ANOVA *via* SPSS 21.0. All the experiments were replicated three times and the mean ± standard deviation (SD) represented the result.

3. Results and discussion

3.1. The structural analysis of zein/ECG complexes

3.1.1. Molecular weight analysis

Two major bands at 21–24 KDa were observed (**Supplementary 1**). As previously reported (Tan et al., 2021), these were the typical bands of α-zein. Additionally, no new bands appeared in zein/ECG complexes (**Supplementary 1B**) compared to zein (**Supplementary 1 A**), indicating that the molecular weight did not increase. No new compounds were formed, and complexes may be formed between zein and ECG mainly by non-covalent binding.

3.1.2. Specific amino acid microenvironment analysis

UV–vis spectroscopy provided insight into the interaction between zein and ECG. Two absorption peaks were observed at 220 nm and 280 nm (Fig. 1A), arising from the peptide bond (C=O) and the tryptophan, tyrosine, and phenylalanine residues of the protein, respectively. The shape of these two peaks remained unchanged after zein was treated with different pH, but the intensities varied.

Upon binding to ECG, the peak intensity of zein increased significantly, demonstrating the formation of zein/ECG complexes. This may be attributed to the overlap of the UV absorption peaks of ECG with these two peaks (Tan et al., 2023). Additionally, the peaks of zein/ECG complexes underwent a slight redshift near 220 nm **(**Fig. 1A**)**. The shift was most pronounced at pH 5, whereas Wang, Tang, et al. (2022c) reported that this occurred at pH 9 between zein and ferulic acid. Moreover, around 280 nm, the peak intensity decreased at pH 7 and 9. This may be evidenced by a certain level of degradation of ECG stability under neutral and alkaline conditions (Peng & Shahidi, 2023).

3.1.3. Secondary structure content analysis

FT-IR spectroscopy can provide structural information about

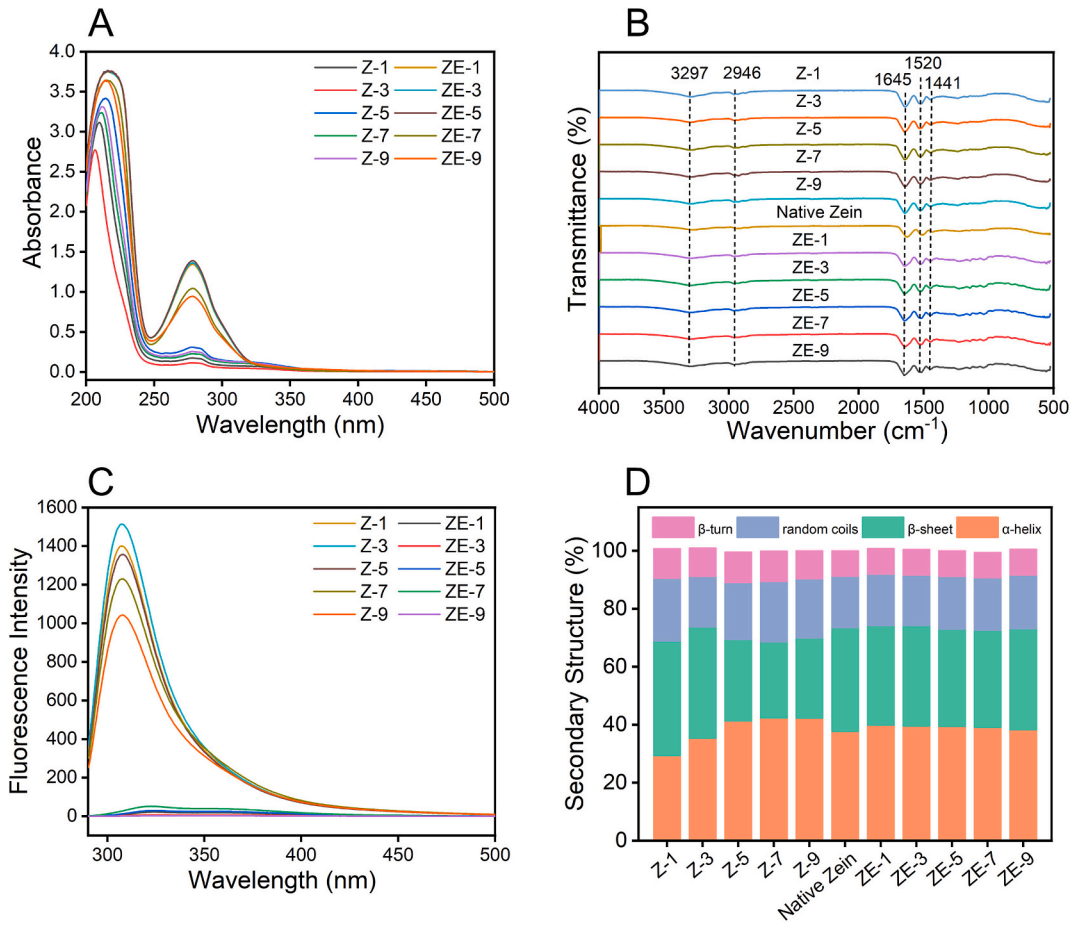

Fig. 1. The spectroscopy characteristics and secondary structure content of zein and zein/ECG complexes at different pH. A: UV–vis spectroscopy; B: FT-IR spectroscopy; C: Intrinsic fluorescence spectroscopy; D: The contents of secondary structure.

proteins (Yang et al., 2020). As shown in Fig. 1B, the characteristic peak of the samples was observed near 3297 cm^{-1}, mainly caused by the -OH stretching vibration (Dong et al., 2023). Around 1600–1500 cm^{-1}, amide II characteristic peaks were observed due to C—N and C═O stretching vibrations. On the other hand, the amide I band (1700–1600 cm^{-1}) was attributed to the combined action of C—N stretching and N—H bending vibrations. It is a reliable indicator for qualitative and quantitative evaluation of the protein's secondary structure. Among them, 1700–1680 cm^{-1}, 1670–1650 cm^{-1}, 1650–1640 cm^{-1}, and 1640–1600 cm^{-1} represent β-turn, α-helix, random coils, and β-sheet, respectively (Zhang et al., 2022).

As shown in Fig. 1D, the α-helix was the most abundant, indicating that it is the main structure of zein, which was consistent with the previous report (Yu et al., 2023). Also, it was observed that the β-sheet content increased after pH 1 and pH 3 treatments. As opposed to that, the β-sheet content decreased while the α-helix increased from pH 5 to pH 9. These changes demonstrate the notable structural alterations that have occurred in zein.

Upon binding to ECG, slight variations in both α-helix and β-sheet content of zein were observed. This suggests that complex formation altered the structure of zein. This result was consistent with the structural alteration of zein induced by EGCG (Liu et al., 2021), and opposite to the effect of ferulic acid on zein structure (Wang, Tang, et al., 2022d). The explanation might be that ECG and EGCG are structurally similar, while they are more different from ferulic acid, thus expressing various effects on zein.

3.1.4. Tertiary structural analysis

In general, intrinsic fluorescence spectroscopy is conducted to assess the alterations in the tertiary structure of protein (Giteru et al., 2021). They are mainly caused by tryptophan (Trp) and tyrosine (Tyr) residues, whose typical maximum emission wavelengths are 348 nm and 304 nm, respectively. These residues are highly sensitive to changes in the surrounding microenvironment. Tyr made a significant contribution to the zein intrinsic fluorescence (Fig. 1C), due to the absence of Trp (Lu et al., 2024), which was consistent with the findings of Liu et al. (2021). Moreover, the intensity reached a maximum of 1514 at pH 3 and decreased to 1038 at pH 9. Presumably, pH altered the microenvironment of these chromophores, leading to a decrease in intensity.

Upon binding to ECG, the emission maxima of zein showed a slight red shift. The intensities were reduced to nearly 50. Thus, the ECG exhibited a fluorescence quenching effect that was not pH-dependent. However, it was reported that the effect of ferulic acid on zein was positively correlated with pH (Wang et al., 2022c). Once again, it was demonstrated that polyphenols have structurally different characteristics and interact with zein in various ways.

3.1.5. Morphological observation analysis

As shown in Fig. 2, zein exhibited spherical particles after undergoing various pH treatments, primarily forming during the slow evaporation of ethanol. As a previous report (An et al., 2016), this process promoted zein self-assembly. Additionally, larger particles were observed at pH 7, compared to pH 1, 3, 5, and 9. Moreover, Li et al. (2023) found that, compared to pH 2 and 4, larger nanoparticles were prepared from zein/proanthocyanidins at pH 7 (red ring marks in Fig. 2). The observed results may be attributed to the weakening of electrostatic repulsion between particles near the zein isoelectric point (pI 6.2), which leads to aggregation. Furthermore, it has been reported

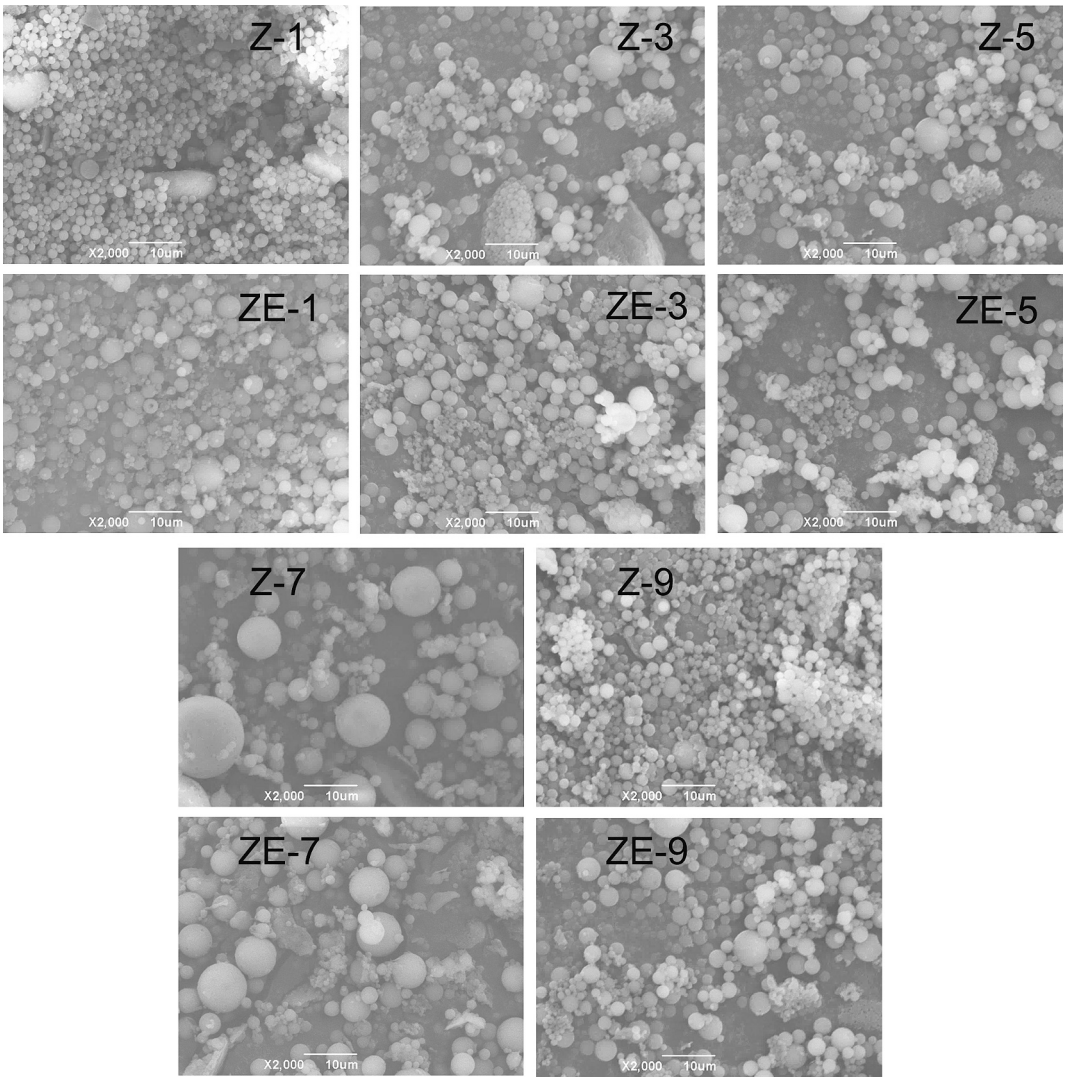

Fig. 2. SEM images of zein and zein/ECG complexes at different pH.

that non-covalent interactions affect self-assembly (Yu et al., 2023). The experiments all demonstrated that pH and interactions with other substances affected the self-assembly of zein, thereby altering particle size.

3.1.6. QCM-D analysis

The present study estimated the binding capacity of ECG to zein under pH 1, 3, 5, 7, and 9, respectively. Figs. 3 **A-E** shows the oscillation frequency (ΔF) and dissipation (ΔD) during the ECG adsorption process on the zein surface. A rise in ΔD indicates that energy in the quartz crystal is quickly released, leading to the creation of a softer or more loosely packed sample film. Conversely, a drop in ΔF implies that the sample is adhering to the chip, which results in a thicker film on the chip.

Most of the changes occurred within the first few minutes, indicating that the sample adsorption is a rapid process. It exhibited similar behavior when treated with pH 1–9. This result is consistent with the adsorption behavior of whey protein (Setiowati et al., 2021). Upon the passage of an ECG solution of the corresponding pH, ΔF decreased rapidly and reached equilibrium within a few minutes, which is similar to the adsorption behavior exhibited by EGCG in bull serum albumin (Wang et al., 2007). However, the equilibrium value of ΔF was greater than ΔF after the adsorption of ECG by zein at all pH conditions except pH 7. The main reason may be the formation of complexes due to the strong interaction between ECG and zein, which are washed out by the buffer and lead to negative adsorption.

The adsorbed mass of zein interacting with ECG under pH 1–9 conditions was shown in Fig. 3F. The mass of ECG adsorbed ($p < 0.05$) onto the surface of zein varied with pH in the following order: pH 9 > pH 1 > pH 3 > pH 5 > pH 7. While the mass reacts to interaction strength, it is hypothesized that there is also a significant difference under different pH conditions. The reasons could be speculated as follows: at pH 1, the phenolic hydroxyl group may exhibit a weak basicity owing to hyperacidity, and the lone pair of electrons on the oxygen can form phenyl oxonium ions with a strong acid (Zheng et al., 2024). It can have strong ionic interactions with the negatively charged amino acids on zein, and this interaction might be shortened because of the weakening of the acidity at pH 3. While at pH 5 and 7, this effect might be greatly weakened due to the proximity of the zein isoelectric point (pI 6.2). However, this effect was indeed enhanced at pH 9, probably because the phenolic hydroxyl group of ECG was ionized to form phenoxy anions or even quinones under this condition (Zhu et al., 2023). They may exhibit stronger interactions with positively charged amino acid ions on zein.

3.1.7. Molecular docking analysis

3.1.7.1. Zein 3D structure prediction. The commercial zein consists mainly of α-zein with two typical bands (21–24 KDa), evidence of which was shown in **Supplementary 1**, indicating that α-zein was the primary

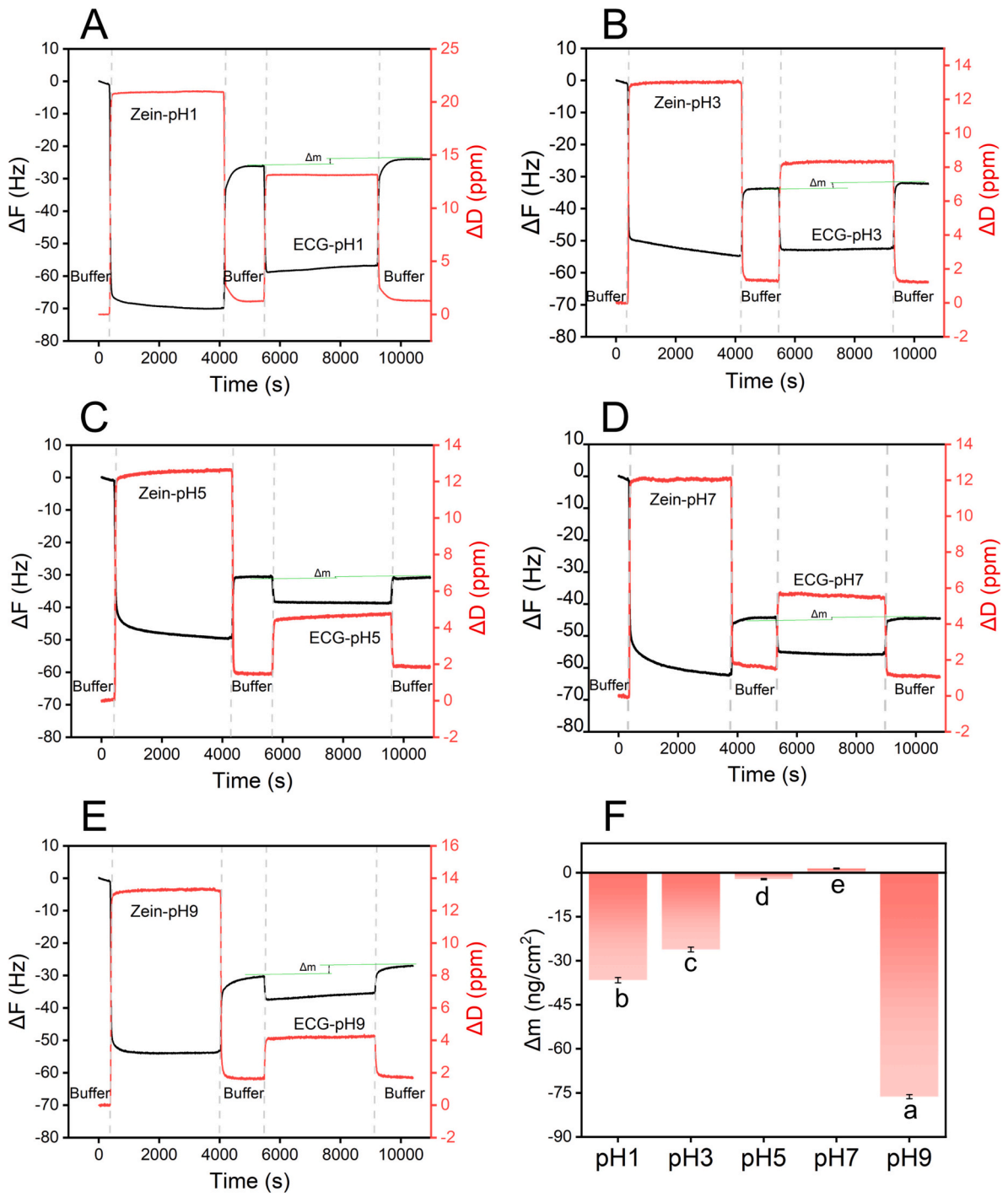

Fig. 3. A-E: Shift in frequency and dissipation from QCM-D measurement of zein and ECG at pH 1, 3, 5, 7, and 9, respectively; F: The adsorption mass of ECG interacting with zein at pH 1, 3, 5, 7, and 9. The various letters mean the presence of notable differences ($p < 0.05$).

material studied. The amino acid sequence of α-zein (22 KDa, UniProtKB: Q9SYT3) was used to construct the zein 3D structure model (Fig. 4B). Additionally, the Ramachandran plot (Fig. 4E) was obtained through PROCHECK analysis. It evaluates the permissible and impermissible conformations of amino acids and is categorized into three main zones. These are the permissive (yellow), core (red), roughly permissive, and forbidden (blank) zones (Park et al., 2023). The percentages of amino acids in these three regions in the zein model constructed in this study were 14.9 %, 84.2 %, and 0.8 %, respectively. Therefore, the zein model adhered to the rules of stereochemistry and was considered reasonable.

Furthermore, the binding site was identified using the POCASA algorithm prediction (https://g6altair.sci.hokudai.ac.jp/g6/service/pocasa/). It was situated at the end of the zein chain segment and was largely formed by chain orientation and folding. The key residues included ALA123, GLN130, GLN156, LEU160, SER162, LEU164, and LEU177, as shown in Fig. 4D.

3.1.7.2. Docking results analysis. Molecular docking has been an important tool for studying the binding conformation of small molecules to proteins. Generally, the binding energy of a protein-small molecule is primarily contributed by intermolecular forces, which mainly include

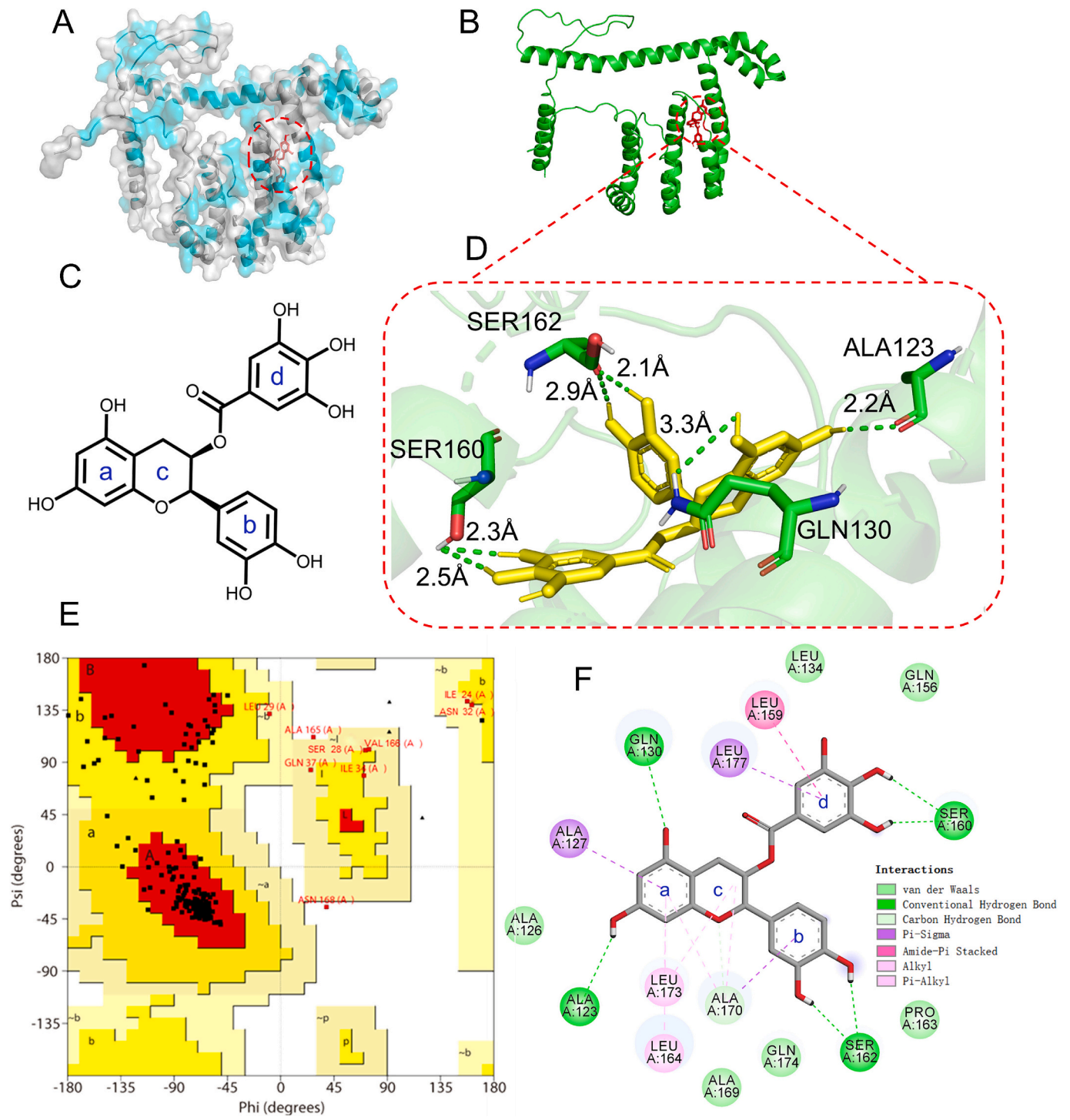

Fig. 4. Diagram of zein and ECG interaction. A: Surface representation of the zein/ECG complex with the lowest binding energy (blue-green cyan represents hydrophilic amino acid residues); B: Carton representation of the zein/ECG complex with the lowest binding energy; C: 2D view of ECG; D: 3D image of binding residues; E: Ramachandran plot for the zein model; F: 2D image of interaction residues. (For interpretation of the references to colour in this figure legend, the reader is referred to the web version of this article.)

hydrogen bonding, van der Waals, ionic bonding, and electrostatic interactions (Zheng et al., 2024). In this study, the formation mechanism of the zein/ECG complex was evaluated by analyzing the conformation with the lowest binding energy. Meanwhile, the zein-ECG interaction forces and the distances between the bound residues were thoroughly investigated.

Binding is more easily induced when the negative binding affinity energy value is less than −6 kcal/mol (Yue et al., 2024). In this study, the lowest binding energy of zein with ECG was −8.07 kcal/mol, indicating a strong binding effect. The binding energies of zein with theaflavin, curcumin, and fucoidan have been reported to be −7.3, −4.0, and − 5.4 kcal/mol, respectively (Lu et al., 2024; Yang et al., 2023). This may be partly attributed to the different structural modeling of zein, coupled with the various structures of small molecules.

Moreover, zein and ECG can bind through hydrophobic interactions and van der Waals forces, since the former is amphiphilic and ECG is

hydrophilic. ECG contains several phenolic hydroxyl groups, which can act as proton donors to form hydrogen bonding interactions with zein. As shown in Fig. 4A, the ECG-bound region is distributed with a large number of polar amino acids such as glutamine, and the ECG binds to the hydrophilic side. ECG is embedded in zein's cavity consisting of multiple amino acid residues and interacts with numerous amino acids (Fig. 4B). Hydrogen bonding, van der Waals forces, and hydrophobic interactions were observed in the complex, details shown in Fig. 4F and **Supplementary 2**. Firstly, the phenolic hydroxyl group of ECG formed strong hydrogen bonding interactions with ALA123, GLN130, SER160, and SER162 reactive groups at distances of 2.2, 3.3, 2.3, 2.5, 2.1, and 2.9 Å, respectively (Fig. 4D). These are strong binding forces and are important for stabilizing ECG in zein. Furthermore, pi-sigma hyperconjugation of the a and d rings of ECG with residues ALA127 and LEU177, respectively, was also observed. Additionally, the d ring of ECG also underwent pi-amide stacking with LEU159 residue (Fig. 4F).

The docking outcomes offer a clear understanding of how ECG and zein prefer to bind together, emphasizing the significant contributions of hydrogen bonds, van der Waals forces, and hydrophobic interactions in the zein/ECG complex. However, ionic interactions were not observed in the optimal conformation, notably because this study did not consider the protonation states of zein and ECG. This is attributed to the protonation state of ECG at different pH conditions, which could not be determined.

3.2. Physicochemical analysis of zein/ECG complexes

3.2.1. Solubility and turbidity analysis

Solubility is a crucial indicator of proteins due to its strong correlation with functions such as gelation and emulsification (Xu et al., 2022a). Zein is a class of proteins rich in nonpolar amino acids with poor water solubility, which limits its application (Fan et al., 2024). The ability of polyphenols to enhance zein solubility through covalent or noncovalent modifications has been reported (Ren et al., 2022; Xu et al., 2022a). As shown in **Fig. 5D**, zein solubility was higher after treatment with pH 9 than the other four pH conditions. The non-hydrophobic amino acids of zein were probably exposed at pH 9, increasing solubility.

Upon binding to ECG, zein solubility increased significantly at pH 1–9, suggesting that ECG strongly interacted with zein. Interestingly, at pH 9, there was no difference in zein solubility with or without ECG. Thus, pH may be the main factor contributing to this situation.

Additionally, the turbidity was appraised by detecting the absorbance value at 600 nm. It was treated at low pH levels of 1, 3, and 5 (**Fig. 5C**) because most of the zein settled to the bottom (red marked in **Figs. 5 A** and **B**). In contrast, the zein treated with pH 7 and 9 exhibited higher turbidity and was more homogeneous in water. Moreover, increasing solubility may be a key factor in improving turbidity (Xu et al., 2022a). Interestingly, in this study, the solubility of zein/ECG complexes at pH 1, 3, and 5 was higher than that of zein without ECG (**Fig. 5D**). Still, the turbidity did not improve (**Fig. 5C**). Therefore, the relationship between solubility and turbidity is worthy of further investigation.

3.2.2. DSC analysis

The melting temperature (Tm) of proteins changes as the protein structure changes (Ren et al., 2022). The various melting temperatures were observed between 77 and 88 °C (Fig. 6). The Tm of zein was 75.14 °C at pH 1 and rose to 79.46 °C at pH 3. However, it dropped to 74.71 °C at pH 7 and then rose to 86.50 °C at pH 9, further demonstrating that pH can influence affect the zein structure.

Upon binding to ECG, the Tm of zein decreased after pH 3, 5, and 9 treatments, suggesting that the structure of zein induced by ECG became

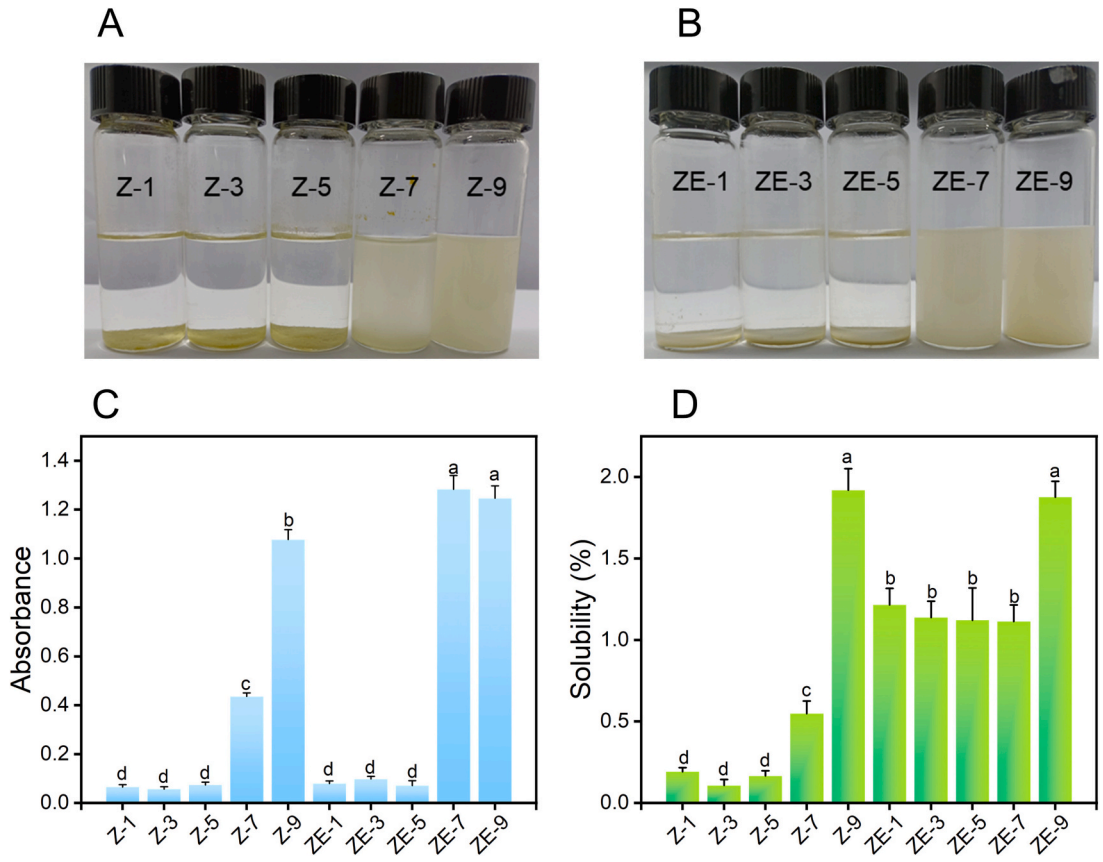

Fig. 5. A and B: Visual observation of the dispersions of zein and zein/ECG complexes at the concentration of 1 mg/mL; C: Turbidity (1 mg/mL) measured on 600 nm; D: Solubility measured in distilled water.

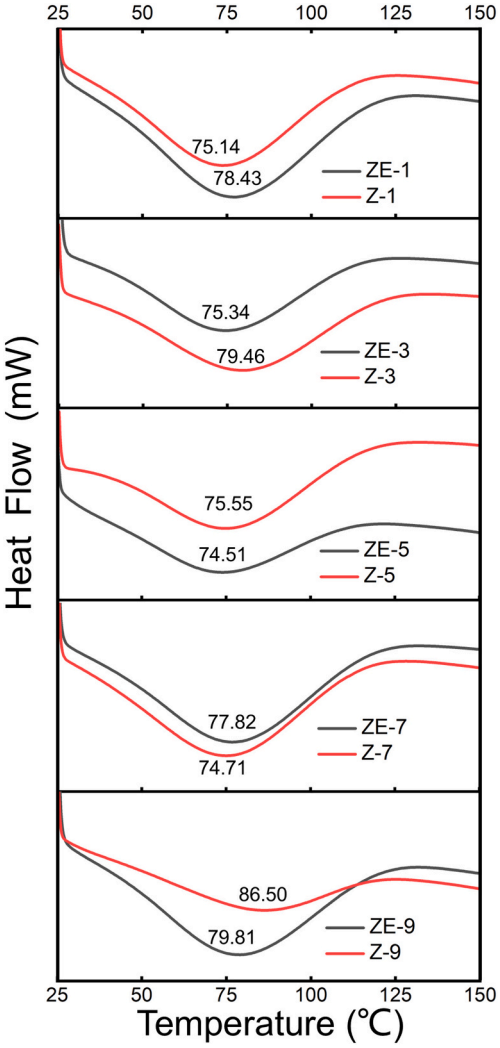

Fig. 6. DSC thermograms of zein and zein/ECG complexes at different pH.

unstable under these conditions. In contrast, the Tm of zein increased by 3 °C at pH 1 and pH 7, respectively. Therefore, ECG might contribute to the structural stabilization of zein under these conditions.

3.2.3. SH content analysis

SH polymerizes proteins through disulfide bonds, which impacts their function and texture (Hong et al., 2024). The SH content of zein and zein/ECG complexes was determined (Table 1). It was treated more effectively under acidic and neutral conditions than under alkaline (pH 9). Presumably, the former conditions might be more favorable for zein SH exposure.

Upon binding to ECG, the SH content of zein was reduced to varying degrees. The SH group exhibited strong nucleophilicity and underwent a nucleophilic substitution reaction with the hydroxyl group of ECG (Zhou et al., 2024), leading to a decrease in SH content. Moreover, the hydroxyl group of ECG could be oxidized to form quinones at pH 9 (Zhu et al., 2023), reducing the nucleophilic attack ability of SH.

Table 1
The free sulfhydryl groups, and scavenging activities on ABTS and DPPH radicals of zein and zein/ECG complexes at different pH.

Samples	Free sulfhydryl groups (μmol/g)	DPPH radical scavenging activity (%)	ABTS radical scavenging activity (%)
Z-1	14.45 ± 1.89^{ab}	26.74 ± 2.34^{c}	56.22 ± 1.71^{c}
Z-3	13.90 ± 0.60^{abc}	20.17 ± 2.09^{d}	53.97 ± 1.12^{c}
Z-5	14.80 ± 0.79^{ab}	26.05 ± 2.72^{c}	59.22 ± 0.91^{b}
Z-7	15.66 ± 0.81^{a}	13.24 ± 1.91^{e}	61.11 ± 0.98^{b}
Z-9	12.77 ± 0.81^{bc}	8.94 ± 1.29^{e}	58.94 ± 0.73^{b}
ZE-1	12.05 ± 1.36^{c}	65.68 ± 3.00^{a}	92.59 ± 1.79^{a}
ZE-3	11.50 ± 1.37^{c}	66.50 ± 3.13^{a}	91.68 ± 2.01^{a}
ZE-5	11.82 ± 0.36^{c}	67.04 ± 1.57^{a}	93.51 ± 0.72^{a}
ZE-7	12.87 ± 0.51^{bc}	63.81 ± 1.39^{a}	92.82 ± 0.66^{a}
ZE-9	11.99 ± 0.71^{c}	55.86 ± 0.66^{b}	92.12 ± 1.16^{a}

Note: In the same column, various letters mean the presence of notable differences ($p < 0.05$).

3.3. Bioactivity analysis of zein/ECG complexes

3.3.1. In vitro antioxidant activity analysis

The DPPH and ABTS radical scavenging activities of zein and zein/ECG complexes were evaluated, and the results are shown in Table 1. Upon binding to ECG, zein's capacity to scavenge DPPH and ABTS radicals was significantly enhanced ($p < 0.05$). The potential explanation might be that ECG had strong antioxidant activity and exhibited this capacity in zein/ECG complexes. This result aligns with the previous report (Yue et al., 2024), where nanoparticles made of zein complexed with quercetin exhibited enhanced antioxidant activity. In addition, the ECG hydroxyl group could be oxidized, reducing the free radical scavenging ability at pH 9. While zein bound to ECG exhibited the strongest scavenging ability for both radicals at pH 5, this finding did not agree with the results of Cao et al. (2018). It was found that whey protein combined with gallic acid and EGCG exhibited the strongest antioxidant activity at pH 7. Thus, the study once again demonstrated the diverse effects of pH on the interaction between various proteins and polyphenols.

3.3.2. In vitro digestion analysis

The simulated digestion behavior of zein and zein/ECG complexes *in vitro* was illustrated in **Figs. 7A** and **B**. Following the pH and ECG modifications, the digestibility of zein continued to be low. Additionally, many previous studies have been conducted to structurally modify zein, but none of them notably improved its digestibility (Wang, Tang, et al., 2022d; Zhao et al., 2022). A previous study found that the primary reason for zein indigestibility was its low water solubility (Calvez et al., 2019). However, as demonstrated in section **3.2.1** of this study, the solubility of zein and zein/ECG complexes at pH 7 and 9 was higher than at pH 1, 3, and 5, without an increase in digestibility. There was also evidence that zein is resistant to pepsin, making it difficult to digest (Wang, Crevel and Mills, 2022). Thus, it is necessary to further explore the reasons for the zein indigestibility indigestibility and to investigate additional modification methods to broaden its application.

4. Conclusion

The present study estimated the changes in the structural and physicochemical properties of zein/ECG complexes prepared under five different pH conditions using multispectral analysis. Additionally, their potential interaction mechanisms were explored through QCM-D and molecular docking. QCM-D analysis revealed that pH significantly influenced the binding capacity of ECG to zein, demonstrating the highest affinity at pH 9. This affinity was notably greater than that observed under the other four acidic and neutral conditions. Molecular docking studies further illustrated the conformation of the zein/ECG complex with the lowest binding energy. Six conventional hydrogen bonds, one carbon-hydrogen bond, van der Waals forces, pi-sigma interaction, pi-alkyl interaction, and amide-pi stacked interaction were identified. Furthermore, ECG interacted with zein, resulting in alterations to the structure and physicochemical properties of zein. ECG promoted tyrosine quenching of zein, as indicated by fluorescence spectroscopy. Slight variations in both α-helix and β-sheet content of zein/ECG complexes were observed after treatment with pH values

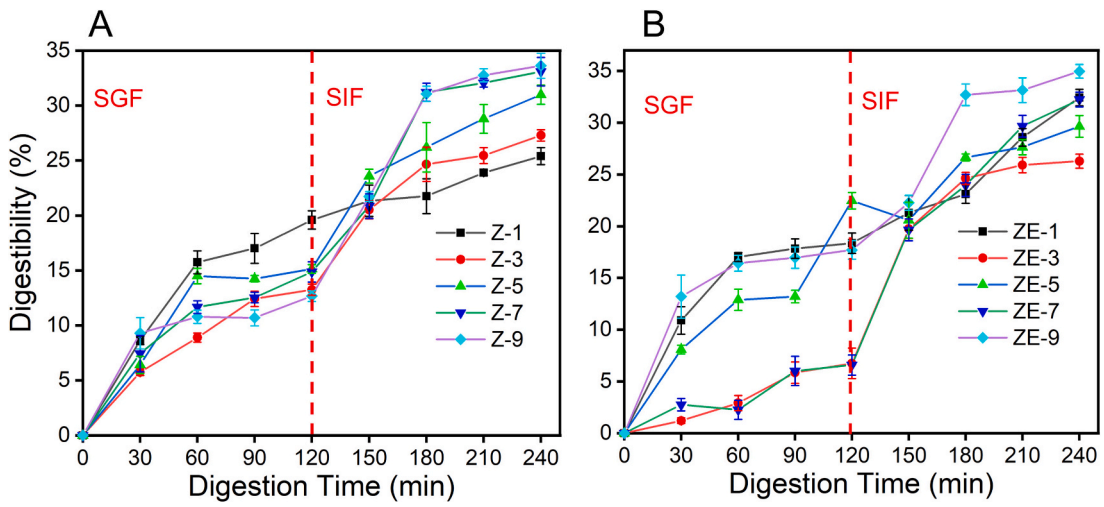

Fig. 7. The digestibility of zein and zein/ECG complexes at different pH.

ranging from 1 to 9. The solubility and antioxidant activity of zein/ECG complexes were significantly enhanced, while the SH content was reduced to different extents. Moreover, upon binding to ECG, the melting temperature of zein decreased after treatments at pH 3, 5, and 9, but increased by 3 °C at pH 1 and pH 7, respectively. Unfortunately, ECG did not exhibit a notable effect on the digestive behavior of zein. This study may offer insights into comprehending the interactions of zein with other micromolecules and the design of zein-based complexes.

CRediT authorship contribution statement

Xiujuan Chen: Writing – original draft, Software, Methodology, Investigation, Data curation, Conceptualization. **Kaili Nie:** Investigation, Data curation. **Xuejun Huang:** Data curation. **Hao Li:** Software, Data curation. **Yexu Wu:** Formal analysis. **Yi Huang:** Validation. **Xiaoqiang Chen:** Writing – review & editing, Visualization, Validation, Resources, Methodology, Funding acquisition, Conceptualization.

Declaration of competing interest

The authors declare that they have no known competing financial interests or personal relationships that could have appeared to influence the work reported in this paper.

Acknowledgment

This research was financially supported by Hubei University talent start-up Fund and the National Natural Science Foundation of China (grant number 31871813).

Appendix A. Supplementary data

Supplementary data to this article can be found online at https://doi.org/10.1016/j.fochx.2024.102028.

Data availability

Data will be made available on request.

References

An, B., Wu, X., Li, M., Chen, Y., Li, F., Yan, X., & Brennan, C. (2016). Hydrophobicity-modulating self-assembled morphologies of α-zein in aqueous ethanol. *International Journal of Food Science and Technology, 51*(12), 2621–2629.

Bu, Y., Fan, M., Sun, C., Zhu, W., Li, J., Li, X., & Zhang, Y. (2024). Study on the interaction mechanism between (−)-epigallocatechin-3-gallate and myoglobin: Multi-spectroscopies and molecular simulation. *Food Chemistry, 448, Article 139208*.

Calvez, J., Benoit, S., Fleury, L., Khodorova, N., Piedcoq, J., Tomé, D., & Gaudichon, C. (2019). True ileal protein digestibility of zein and whey protein isolate in healthy humans (OR27-06-19). *Current developments. Nutrition, 3*. nzz046.OR027-006-019.

Cao, Y., Xiong, Y. L., Cao, Y., & True, A. D. (2018). Interfacial properties of whey protein foams as influenced by preheating and phenolic binding at neutral pH. *Food Hydrocolloids, 82*, 379–387.

Chen, D., Stone, S., Ilavsky, J., & Campanella, O. (2024). Effect of polyphenols on the rheology, microstructure and *in vitro* digestion of pea protein gels at various pH. *Food Hydrocolloids, 151, Article 109827*.

Dong, L., Jiao, Q., Gao, J., Luo, X., Song, Y., Li, T., & Luo, Z. (2023). Effects of zein-lecithin-EGCG nanoparticle coatings on postharvest quality and shelf life of loquat (*Eriobotrya japonica*). *LWT-food. Science and Technology, 182, Article 114918*.

Fan, S., Yang, Q., Wang, D., Zhu, C., Wen, X., Li, X., & Zhang, D. (2024). Zein and tannic acid hybrid particles improving physical stability, controlled release properties, and antimicrobial activity of cinnamon essential oil loaded Pickering emulsions. *Food Chemistry, 446, Article 138512*.

Giteru, S. G., Ali, M. A., & Oey, I. (2021). Recent progress in understanding fundamental interactions and applications of zein. *Food Hydrocolloids, 120, Article 106948*.

Guo, X., Wei, Y., Liu, P., Deng, X., Zhu, X., Wang, Z., & Zhang, J. (2024). Study of four polyphenol-*Coregonus peled* (*C. Peled*) myofibrillar protein interactions on protein structure and gel properties. *Food chemistry: X, 21*. , article 101063.

Hong, T., Tan, Z., Yang, T., Xu, D., Jin, Y., Wu, F., & Xu, X. (2024). Dynamic behavior of zein-gluten interaction during extruded noodle processing. *Food Hydrocolloids, 147, Article 109320*.

Li, S., Wang, X., Zhang, X., Zhang, H., Li, S., Zhou, J., & Fan, L. (2023). Interactions between zein and anthocyanins at different pH: Structural characterization, binding mechanism and stability. *Food Research International, 166, Article 112552*.

Liu, C., Lv, N., Ren, G., Wu, R., Wang, B., Cao, Z., & Xie, H. (2021). Explore the interaction mechanism between zein and EGCG using multi-spectroscopy and molecular dynamics simulation methods. *Food Hydrocolloids, 120, Article 106906*.

Liu, F., Ma, C., McClements, D. J., & Gao, Y. (2017). A comparative study of covalent and non-covalent interactions between zein and polyphenols in ethanol-water solution. *Food Hydrocolloids, 63*, 625–634.

Lu, Y., Cai, X., Lv, W., Duan, C., Li, X., Ma, F., & Li, D. (2024). Multispectral analysis and molecular docking to predict the mechanism of molecular interactions of curcumin, zein and fucoidan complexes. *Journal of Food Engineering, 369, Article 111953*.

Park, S. W., Lee, B. H., Song, S. H., & Kim, M. K. (2023). Revisiting the Ramachandran plot based on statistical analysis of static and dynamic characteristics of protein structures. *Journal of Structural Biology, 215(1), Article 107939*.

Peng, H., & Shahidi, F. (2023). Oxidation and degradation of (epi)gallocatechin gallate (EGCG/GCG) and (epi)catechin gallate (ECG/CG) in alkali solution. *Food Chemistry, 408, Article 134815*.

Ren, G., Shi, J., Huang, S., Liu, C., Ni, F., He, Y., & Xie, H. (2022). The fabrication of novel zein and resveratrol covalent conjugates: Enhanced thermal stability, emulsifying and antioxidant properties. *Food Chemistry, 374, Article 131612*.

Ruan, C., Nian, Y., Chen, Q., Li, N., He, X., Li, C., & Hu, B. (2022). Higher affinity of polyphenol to zein than to amyloid fibrils leading to nanoparticle-embed network wall scaffold to construct amyloid fibril-zein-EGCG hydrogels for coating of beef. *Food Research International, 156, Article 111187*.

Setiowati, A. D., De Neve, L., A'Yun, Q., & Van der Meeren, P. (2021). Quartz crystal microbalance with dissipation (QCM-D) as a tool to study the interaction between whey protein isolate and low methoxyl pectin. *Food Hydrocolloids, 110, Article 106180*.

Tan, H., Zhou, H., Guo, T., Zhang, Y., & Ma, L. (2021). Integrated multi-spectroscopic and molecular modeling techniques to study the formation mechanism of hidden zearalenone in maize. *Food Chemistry, 351, Article 129286*.

Tan, J., Vincken, J.-P., van Zadelhoff, A., Hilgers, R., Lin, Z., & de Bruijn, W. J. C. (2023). Presence of free gallic acid and gallate moieties reduces auto-oxidative browning of epicatechin (EC) and epicatechin gallate (ECg). *Food Chemistry, 425, Article 136446*.

Vale, E. P., Tavares, W., & d. S., Hafidi, Z., Pérez, L., Morán, M. d. C., Martin-Pastor, M., & Sousa, F. F. O. d.. (2024). Epigallocatechin-3-gallate loaded-zein nanoparticles: Molecular interaction, antioxidant, antienzimatic, hemolytic and cytotoxic activities. *Journal of Molecular Liquids, 394, Article 123718*.

Wang, J., Yu, Z., Wu, W., He, S., Xie, B., Wu, M., & Sun, Z. (2022). Molecular mechanism of epicatechin gallate binding with carboxymethyl β-glucan and its effect on antibacterial activity. *Carbohydrate Polymers, 298, Article 120105*.

Wang, K., Crevel, R. W. R., & Mills, E. N. C. (2022). Assessing protein digestibility in allergenicity risk assessment: A comparison of in silico and high throughput *in vitro* gastric digestion assays. *Food and Chemical Toxicology, 167, Article 113273*.

Wang, Q., Tang, Y., Yang, Y., Lei, L., Lei, X., Zhao, J., & Ming, J. (2022c). The interaction mechanisms, and structural changes of the interaction between zein and ferulic acid under different pH conditions. *Food Hydrocolloids, 124, Article 107251*.

Wang, Q., Tang, Y., Yang, Y., Lei, L., Lei, X., Zhao, J., & Ming, J. (2022d). Interactions and structural properties of zein/ferulic acid: The effect of calcium chloride. *Food Chemistry, 373, Article 131489*.

Wang, X., Ho, C., & Huang, Q. (2007). Investigation of adsorption behavior of (−)-epigallocatechin gallate on bovine serum albumin surface using quartz crystal microbalance with dissipation monitoring. *Journal of Agricultural and Food Chemistry, 55*(13), 4987–4992.

Xu, Y., Wei, Z., & Xue, C. (2023). Pickering emulsions stabilized by zein–gallic acid composite nanoparticles: Impact of covalent or non-covalent interactions on storage stability, lipid oxidation and digestibility. *Food Chemistry, 408*. Article 135254.

Xu, Y., Wei, Z., Xue, C., & Huang, Q. (2022a). Assembly of zein-polyphenol conjugates via carbodiimide method: Evaluation of physicochemical and functional properties. *LWT-food. Science and Technology, 154, Article 112708*.

Xu, Y., Wei, Z., Xue, C., & Huang, Q. (2022b). Covalent modification of zein with polyphenols: A feasible strategy to improve antioxidant activity and solubility. *Journal of Food Science, 87*(7), 2965–2979.

Yang, T., Tao, G., Li, L., & Ma, Q. (2023). Study of the interaction mechanism between theaflavin and Zein. *Journal of Food Engineering, 359, Article 111700*.

Yang, X., Bi, Z., Yin, C., Zhang, S., Song, D., Huang, H., & Li, Y. (2024). A colorimetric sensor array based on peroxidase activity nanozyme for the highly efficient differential sensing of tea polyphenols and Tieguanyin adulteration. *Food Chemistry, 432, Article 137265*.

Yang, Y., Wang, Q., Lei, L., Li, F., Zhao, J., Zhang, Y., & Ming, J. (2020). Molecular interaction of soybean glycinin and β-conglycinin with (−)-epigallocatechin gallate induced by pH changes. *Food Hydrocolloids, 108, Article 106010*.

Ye, J., Zhang, Y., & Meng, J. (2022). Protein–ligand interactions for hydrophobic charge-induction chromatography: A QCM-D study. *Applied Surface Science, 572, Article 151420*.

Yu, Y., Li, S., Xu, T., Huang, G., & Xiao, J. (2023). Assembly of zein/propylene glycol alginate nanoparticles in aqueous ethanol and the binding kinetics. *Food Hydrocolloids, 139, Article 108545*.

Yue, X., Xu, P., Luo, X., & Zhao, B. (2024). Multi-spectroscopies and molecular docking insights into the interaction mechanism and antioxidant activity of isoquercetin and zein nanoparticles. *International Journal of Biological Macromolecules, 263, Article 130412*.

Zhang, X., Gao, M., Zhang, Y., Dong, C., Xu, M., Hu, Y., & Luan, G. (2022). Effect of plasticizer and zein subunit on rheology and texture of zein network. *Food Hydrocolloids, 123, Article 107140*.

Zhao, C., Li, Q., Hu, N., Yin, H., Wang, T., Dai, X., & Liu, J. (2022). Improvement of structural characteristics and *in vitro* digestion properties of zein by controlling postharvest ripening process of corn. *Food Control, 142, Article 109221*.

Zheng, J., Li, Y., Zhao, S., Dong, G., Yi, S., & Li, X. (2024). Inhibition effect of epicatechin gallate on acid phosphatases from rainbow trout (*Oncorhynchus mykiss*) liver by multispectral and molecular docking. *International Journal of Biological Macromolecules, 261, Article 129794*.

Zhou, H., Shang, X., Li, W., Zhu, C., Yang, G., & Dou, Y. (2024). Oxidative dehydroxycyclization of catechols with *o*-mercaptoanilines to access 1-hydroxyphenothiazines. *Journal of Organic Chemistry, 89*(7), 4768–4773.

Zhu, M., Fei, X., Gong, D., & Zhang, G. (2023). Effects of processing conditions and simulated digestion *in vitro* on the antioxidant activity, inhibition of xanthine oxidase and bioaccessibility of epicatechin gallate. *Foods, 12*(14), 2807.